Probabilistic soil model for seismic risk assessment based on SDMT results

Yeudy F. Vargas-Alzate[1#], *Dani* Tarragó[1], *Ana M* Zapata-Franco[1] and *Antonio* Gens[1]

[1]*Universitat Politècnica de Catalunya, Department of Civil and Environmental Engineering, Jordi Girona 1-3, Spain*
[#]*Corresponding author: yeudy.felipe.vargas@upc.edu*

ABSTRACT

A new geotechnical site investigation has been conducted in the southern breakwater basin of the Port of Barcelona, for which hundreds of in-situ and lab tests have been performed. Among these tests, this study focuses on the evaluation of triple points. That is, at the prospected locations, there are results from seismic dilatometer Marchetti test (SDMT), cone penetration tests (CPTu), and laboratory tests based on soil samples. Based on this information, the probabilistic distribution of the dynamic and geometrical properties of the soil profiles can be properly characterized. Eleven closely spaced boreholes have been used to characterise the statistical properties of the input variables. The objective of this article is twofold. First, the probabilistic generation of one-thousand soil profiles, which are statistically compatible with the data provided by the eleven aforementioned boreholes. Secondly, to analyse how the elastic properties of the generated soil profiles evolve once seismic waves have passed through them. To do so, a large set of ground motion recorded in hard soils have been employed. Results show that the dynamic response of the soil can be properly parametrized if considering intensity measures extracted from the ground motions acting at the bedrock level. From the results obtained, fragility functions have been derived for risk assessment purposes.

Keywords: Marchetti dilatometer tests; site effects; soil dynamic properties; equivalent linear method.

1. Introduction

The dynamic response of the soil in front of seismic actions is a complex nonlinear phenomenon involving several random variables (Pitilakis and Petridis 2022). This complexity stems from the type of rupture, proximity to the epicenter and depth, site conditions and the mechanical properties of the media through which the seismic waves pass. In addition, depending on the depth, these waves modify the mechanical properties of the soil at very low shear strains (Okur and Ansal 2007); the deeper, the lesser the variation. Consequently, a proper modelling of the seismic response of near-surface soils must therefore considers the randomness of the implied variables and the non-linearities.

Understanding the dynamic response of the soil beneath a civil structure is crucial for seismic risk studies. It is because this soil acts as an ultimate filter by amplifying or damping harmonics depending on its dynamic properties (Cruz and Miranda 2021).

Due to the importance (and sometimes because of its complexity) of the civil structures, it is necessary to analyze its seismic interaction with the soil beneath using advanced nonlinear models. In this respect, advanced nonlinear analysis considering 3D FEM-based representations, offer valuable insights into this problem. However, for computational efficiency, simplified 1D models like Kelvin-Voigt solids, which effectively approximate soil dynamics, are often used (Hardin and Scott 1967).

In this research, data from an extensive marine geotechnical investigation have been used to characterize the soft soils of the Port of Barcelona delta. The scope included 132 continuous rotary boreholes, 168 Cone Penetration Tests (CPTU) with pore pressure measurements, 11 seismic dilatometer Marchetti test (SDMT), and a comprehensive laboratory testing program. Additionally, 11 triple-point locations have been selected for integrated tests to minimize soil disturbance (CPTu, SDMT and Borehole).

This research uses data from the described geotechnical investigation to analyze how the propagation of seismic waves through random soil profiles affects their dynamic properties. These profiles have been simulated to be statistically compatible with those derived from the geotechnical characterisation carried out at the Port. To do so, it has been employed a computational framework originally intended to assess seismic risk in civil infrastructures (Zapata-Franco et al. 2023). It allows to consider the randomness related to the seismic hazard and the mechanical properties of both soil and civil structures. However, the main focus of this research is to study the causal relationship between the main features of the ground motions in terms of intensity measures (IMs) and engineering demand parameters of the soil (EDPs).

Several implementations, mainly in terms of the random generation and the degradation of soil profiles, have been performed to enhance the original computational framework developed in (Zapata-Franco et al., 2023); these implementations allow considering: i) diverse geological conditions; ii) variation in the type of

materials; iii) non-uniform distribution of materials with depth; and iv) the pairing between number of records and soil profiles should not be biunivocal. These improvements allow for a more comprehensive exploration of the relationship between IMs and EDPs. Hence, the seismic risk of the special facilities located in the Port can be adequately characterised.

2. Probabilistic soil model

A probabilistic soil model is used in geotechnical applications to consider the spatial (Vanmarcke 1977) and temporal (Carrière et al. 2018) variability of soil properties. The objective is to measure how these uncertainties influence the dynamic response of civil structures. The randomness of soil properties (e.g. stiffness and damping) are simulated using statistics methods and laboratory tests. As commented above, this paper adopts the computational framework presented in Zapata-Franco et al., 2023, which allows for:

a) Random generation of the dynamic features of the modelled soil profile (G_i, ρ_i, ξ_i and h_i stand for shear modulus, density, damping and layer thickness, respectively).
b) Introduce a ground motion record at the bedrock level of a probabilistically simulated soil profile.
c) Estimate the stiffness degradation and increase of damping of each soil layer based on the equivalent linear method.
d) Calculate the resulting ground motion at the surface after propagating through the soil profile, considering the degradation of soil properties.
e) The resulting ground motion estimated in the previous step acts at the base of a probabilistic building model.

It is worth mentioning that this study does not consider the generation of buildings (Step e). Instead, the main objective is on investigating the causal relationship between IMs and EDPs; these latter are extracted from the dynamic response of the soil profile.

In order to improve the consistency of the simulated soil profiles with the real condition, several improvements have been made to the original computational framework. In particular, the standard deviation, which represents the level of variability of soil properties, has been incorporated as a depth-dependent parameter. Moreover, the interaction of different types of materials can be considered within the soil profile, recognising its high heterogeneity. This also allows to consider the distribution of materials as a function of depth, providing an accurate representation of the evolution of material properties.

Another notable improvement is with respect to the restriction of having the same number of seismic signals and soil profiles. This adjustment significantly improves the practicality and usefulness of the computational framework, facilitating its employment in situations where obtaining seismic signals is difficult or impractical. This increased adaptability makes it a versatile tool for comprehensive risk assessments in a variety of geological contexts.

2.1. Case of study

2.1.1. On-site and laboratory tests

Increasingly, there is a need to perform seismic response analyses of foundation soils, for which the shear wave velocity, Vs, serves as a fundamental input parameter. Several seismic codes and regulations (e.g. API, 2014; BSSC, 2021; Eurocode 8, 2004) recommend determining Vs at least within the first 30 meters of depth for construction projects located in seismic zones.

This article focuses on the results obtained from SDMT tests coinciding with the triple-point locations. From the entire set of results, it has been used the Vs obtained through SDMT and the basic soil identification based on laboratory tests. The SDMT is an evolution of the flat dilatometer Marchetti test (DMT) developed by S. Marchetti, 1980. In the SDMT, seismic sensors are incorporated to measure shear wave velocities (D. Marchetti 2018). The SDMT is equipped with two receivers located at a distance of 0.5 meters. When a shear wave is generated on the seabed surface from the source, it first reaches the upper receiver (blue) and then, after a delay, the lower receiver (red). The Vs is obtained as the difference in distances between the source and the two receivers (S2 - S1), divided by the delay, Δt, between the first and second receiver (see Figure 1). The seismograms generated by the two receivers, which are amplified and digitized at depth, allow for the determination of Δt (see Figure 1) (S. Marchetti, Marchetti, and Villalobos 2013).

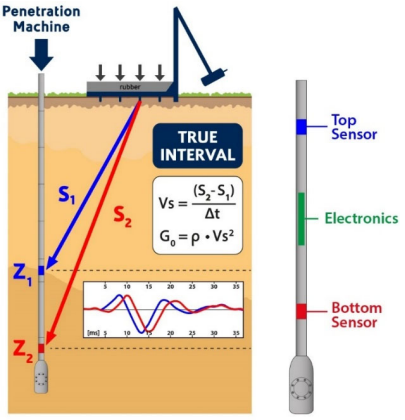

Figure 1. Diagram of SDMT, Marchetti (2018).

The SDMT allows for the determination of the maximum stiffness, G_0, under small strains. On the other hand, stiffness under service conditions can be represented by the modulus of deformation (M_{DMT}). These two stiffness values can guide the selection of degradation curves G-γ, which describe the reduction in shear modulus G as a function of shear strain γ. Amoroso, et al., 2012 present this methodology and define ranges where it is possible to intersect the measured data of G_0 and MDMT with previously available degradation curves. Additionally, using Vs values for clean sands, it can be estimated the potential for cyclic liquefaction by evaluating the cyclic resistance ratio (CRR) using appropriate curves (Andrus & Stokoe, 2000).

2.1.2. Characterization of soil profiles

Based on the geophysical tests described in the previous section, a compilation of 11 soil profiles with different stratigraphy, and depths ranging from 37m to 40.5m, has been made (See Figure 2). From the laboratory and in-situ tests results, three main groups of materials that are characteristic of continental shelf soils have been found in the study area. In the upper strata, there is a large presence of silty sands with some intrusions of organic material, whose thicknesses vary between 0.5m and 2m. In the middle layers, there is a large presence of silty clays. In the lower layers, there is a large amount of clayey material with some intrusions of organic material. This material heterogeneity has been considered in the generation of soil profile samples. The profiles shown in Figure 2 are a representative and detailed sample of the dynamic properties of the soil in the study area. The information derived from them has been used in the subsequent simulations.

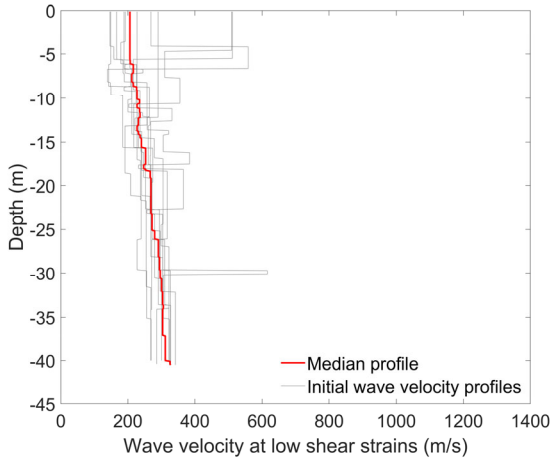

Figure 2. Soil profiles obtained from the geophysical exploration

2.2. Probabilistic generation of soil profiles

The probabilistic framework used in this research employs the Toro's model to generate random soil profiles (Silva et al. 1996). This model incorporates three main elements: i) information describing the random stratigraphy at the site; ii) the median wave velocity profile; iii) the dispersion of the Vs with depth and the correlation between consecutive layers.

2.2.1. Random stratigraphy at the site

The results of the geotechnical investigations carried out in the Port of Barcelona have been used to characterize the random stratigraphy at the site. The "Layering Model" has been employed (Silva et al. 1996), which allows to consider that as the layer is deeper, it becomes thicker. Thus, for each layer and respective depth from the soil profiles depicted in **Figure 2**, a cloud of transition points has been statistically parametrized. The following power law has been adopted:

$$\lambda(h) = C_3[h + C_1]^{-C_2} \qquad (1)$$

where λ is the layer boundary rate (i.e. the inverse of the thickness of the layer, 1/m) and h is the depth in the middle point of the layer in m. The estimation of the values C_1, C_2 and C_3 is carried out by using the capabilities of the Monte Carlo method to minimize multi-dimensional functions. Figure 3 shows this statistical parametrization. Using the regression line, and by considering the dispersion of the data, the geometrical random features of the stratigraphy have been considered in the generated soil profiles.

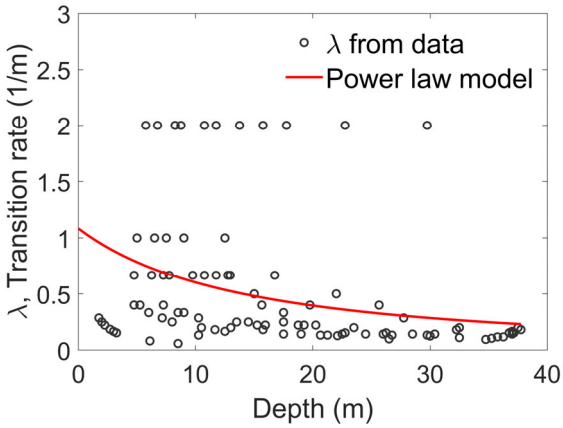

Figure 3. Relationship between the transition rate and depth

2.2.2. The median wave velocity profile at the site

The median velocity profile shown in Figure 2 has been used to generate random soil profiles. Due to the cumulative process associated with marine deposits, it has been observed that a log-normal distribution parametrizes adequately the aleatory character of shear wave velocities (Toro 2022). This distribution has been adopted in the sampling process of this variable.

2.2.3. Deviations of the velocity in each layer and correlation between consecutives layers

From the base profiles shown in Figure 2, it has been estimated how the standard deviation changes with depth. In the analyzed case, it can be observed that this variable tends to decrease with depth. This feature has been incorporated in the random generation of profiles.

Another important aspect observed in soil profiles is related to the spatial correlation between closer layers. The closer the layers the higher the correlation (Angelini and Heuvelink 2018). This implies that widely separated layers tend to be less correlated. It has been assumed that the correlation between adjacent soil layers decreases with distance by means of the following conditions:

$$\rho_{i,j} = \begin{cases} i = j & \rho_{i,j} = 1 \\ i = j \pm k & \rho_{i,j} = 1 - \dfrac{k}{r} \geq 0 \end{cases} \qquad (2)$$

where k is a number related to the position of a layer belonging to the same profile; r is a coefficient associated to the rate of correlation between adjacent layers. In this research, r has been fixed to 100/3.

2.3. Probabilistic simulation of soil profiles

Based on the description of the probabilistic features that must meet the soil profiles, one-thousand statistic realizations of them have been performed via Monte Carlo simulation. The resulting soil profiles for shear

wave velocity can be seen in Figure 4. It is worth mentioning that they correspond to low shear strains.

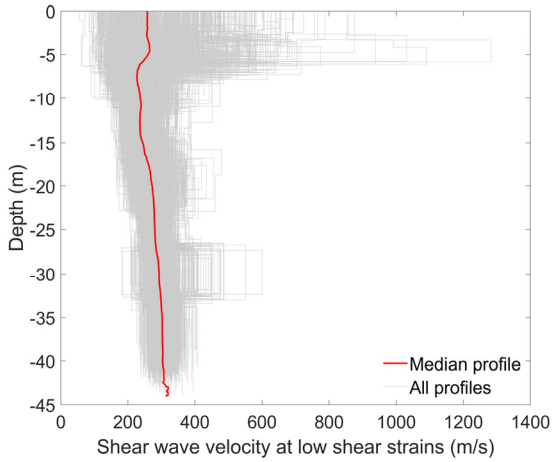

Figure 4. Probabilistic shear wave velocity profiles

The damping properties at low shear strains have been obtained by using degrading curves for the soil types analyzed. In general, these values vary in a narrow band between 1-1.2 %. Another important variable influencing the dynamic properties of the simulated soil profiles is density (ρ). This variable is calculated from the unit weight (γ). It has been considered as a random variable by using the relationship proposed in Nakamura, 1989:

$$\gamma = 8.32 \cdot \log_{10} Vs - 1.61 \cdot \log_{10} H \qquad (3)$$

where H is the depth in m. Figure 5 depicts the random set of ρ profiles after applying Eq (3).

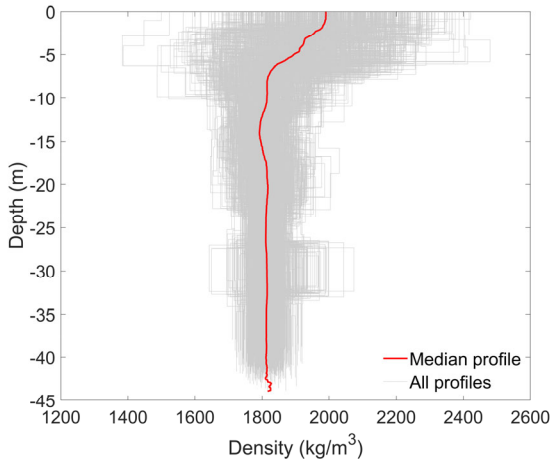

Figure 5. ρ of the soil profiles

Once the probabilistic set of soil profiles has been generated, it is necessary to characterise the seismic hazard at the site. It has been done by considering ground motion records acquired in seismic stations. Then, using both soil profiles and ground motion records, the probabilistic propagation of seismic waves can be performed.

3. Seismic hazard characterization

The study of earthquake-induced ground vibrations has become a topic of great importance, not only in areas of high seismic hazard, but worldwide. This is due to the fact that, as commented in (Coburn and Spence 2002), earthquakes with magnitudes around 5.5 Mw can occur almost anywhere in the world (this represents the level of energy that can be released in non-tectonic geological processes). If these events are shallow, and trigger significant intensities in areas containing vulnerable structures, they can cause great damage. Evidence of this has been provided by (Alarcón and Benito Oterino 2014), who analyzed the negative consequences of two earthquakes on the civil infrastructure of several European cities, particularly *Lorca* in Spain and *Emilia* in Italy. What is most notable about these catastrophic events is that the related earthquakes can be considered low-to-moderate magnitude (5.1 and 5.8 Mw, respectively). This situation is not unique to Europe; several regions of the world are highly vulnerable to earthquakes, especially in low-income areas.

In line with the above, instead of using probabilistic seismic hazard calculations to characterize the expected ground motions of the area, which may derive in underestimation of the expected risk (Mulargia, Stark, and Geller 2017), it has been opted to select earthquakes whose magnitude range between 4 and 6 Mw; the maximum hypocentral distance has been set at 10 km. The Engineering Strong Motion Database has been used to select these ground motion records (Luzi, Puglia, and Russo 2016). Figure 6 shows the spectra of the 125 signals that met the requirements described above.

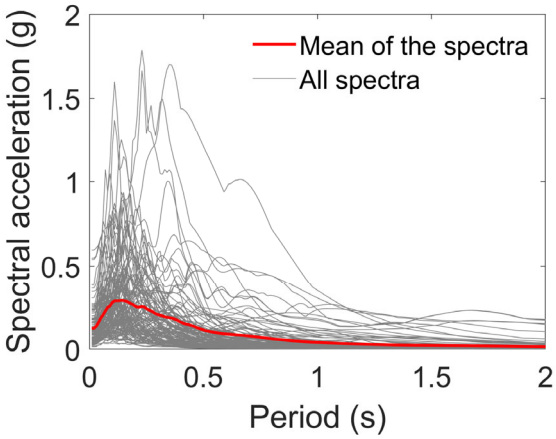

Figure 6. Spectra of 125 selected ground motion records

4. Degradation of soil properties

Depending on the soil type and depth, the mechanical properties of the soil can be highly modified due to the pass of seismic waves. In this respect, it is a common practice to use simplified 1D soil models to 3D finite-element representations. However, the higher the complexity of the model the higher the computational time involved in solving the dynamic problem. In addition, due to the boundary conditions related to the reflection of the seismic waves, it is sometimes necessary to develop large soil models, which significantly increase the number of finite elements.

In order to tackle the computational effort related to 3D models, simplified soil representations are widely used to estimate the dynamic response of large simulations. One of the most employed is the 1D model,

in which the soil layers are considered as Kelvin-Voigt solids. This model is represented by a purely viscous damper and elastic spring connected in parallel. It allows a good approximation of the dynamic response of a soil volume. Moreover, this model has been extended to consider nonlinearities associated to the stiffness degradation of the soil, and the consequent increase in damping due to shear strains. It can be achieved by means of the linear equivalent method (Assimaki, Kausel, and Whittle 2000). The 1D model becomes an ideal candidate to include uncertainties via Monte Carlo simulations.

Using the methodology described above, the propagation of seismic waves through the soil profiles is carried out. Figure 7 shows in grey the one-thousand nonlinear wave velocity profiles after the degradation process whilst the red one shows the median profile. Comparing the fundamental period of the elastic and inelastic median profiles (See Figure 8), it can be seen a significant degradation of the stiffness.

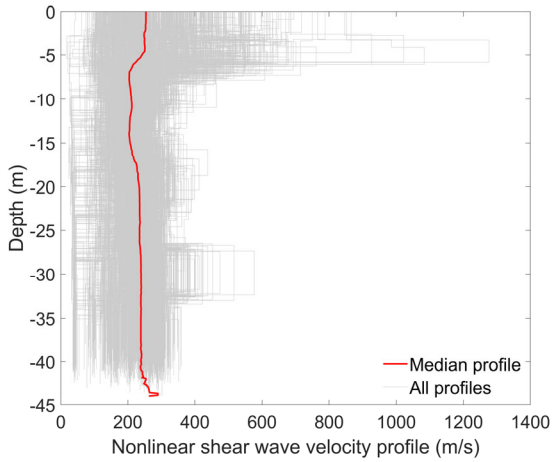

Figure 7. Nonlinear Vs of the one-thousand profiles

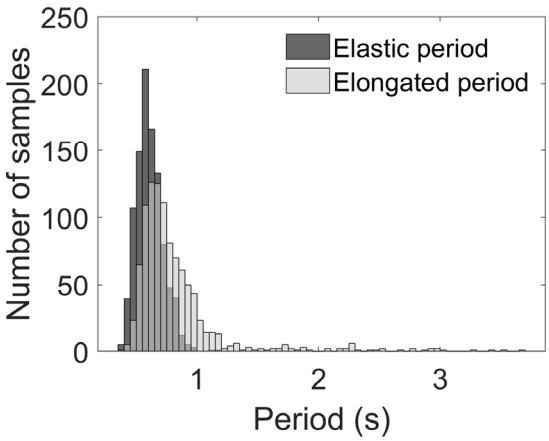

Figure 8. Comparison between the elastic and inelastic fundamental periods

The median of the ratios between the elongated and elastic periods is around 16%. Regarding damping, it has been observed that, after the propagation process, the median profile is around 5%. Note that the damping tends to increase with depth. It can be related with the materials found in the study zone.

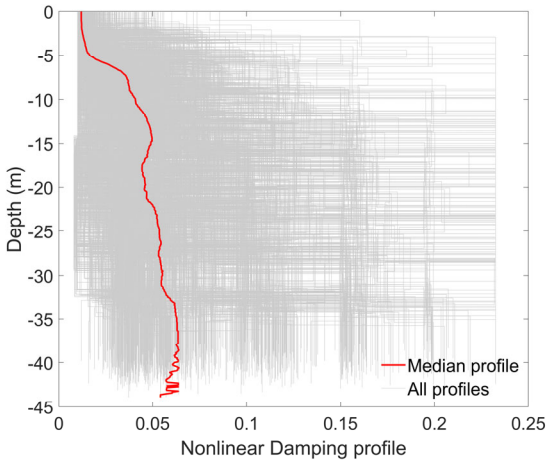

Figure 9. Nonlinear damping of one-thousand profiles

5. Intensity measures and engineering demand parameters

The relationship between IM and EDPs can be employed to estimate the expected risk of systems. For instance, from a set of IM-EDP pairs, one can derive fragility functions according to the so-called 'cloud analysis' approach (Jalayer, De Risi, and Manfredi 2015).

5.1. Intensity measures

An instrumental IM is a parameter extracted from a ground motion record to characterize seismic hazard (Atkinson and Kaka 2007). In this article, a set of 18 IMs have been employed. They have been summarized in **Table *1***; further details on how to calculate them can be found in Vargas-Alzate et al., 2022.

Table 1. Intensity measures

Intensity Measure	Variable
Spectral acceleration at T_1	$Sa(T_1)$
Spectral velocity at T_1	$Sv(T_1)$
Spectral displacement at T_1	$Sd(T_1)$
Average spectral acceleration	$AvSa$
Average spectral velocity	$AvSv$
Average spectral displacement	$AvSd$
Equivalent velocity at T_1	$VE(T_1)$
Average equivalent velocity	$AvVE$
Peak ground acceleration	PGA
Peak ground velocity	PGV
Peak ground displacement	PGD
Specific Energy Density	SED
Arias intensity	I_A
Characteristic intensity	I_C
Root mean of the velocity	vel_{RMS}
Root mean of the acceleration	acc_{RMS}
Cumulative Absolute Velocity	CAV
Fajfar intensity	I_F

*T_1, *is the fundamental period* (s)

5.2. Engineering demand parameters

EDPs are variables extracted from the dynamic response of systems, and can be used to characterize the expected damage. In this article, three EDPs have been

analyzed: i) the maximum shear strain reached by the soil profile, γ_{max}; ii) the elongation of the fundamental period of the soil profile, δT; iii) the resulting damping after the wave propagation, ξ.

5.3. IM-EDP pairs and fragility functions

Two types of regression models have been employed to parametrize the IM-EDP relationship (linear and non-linear). The reason for considering a non-linear regression model is that, in some cases, this relationship cannot be properly described by using linear functions. Further details on both type of regression models can be found in (Vargas-Alzate, Hurtado, and Pujades 2022).

There are several ways to derive fragility functions by using IM-EDP pairs. Note that these curves are used to define the probability of exceedance a given damage threshold. The latter is a specific value of the EDP under consideration. For instance, in cloud analysis (Jalayer, De Risi, and Manfredi 2015), a best fit curve between a set of IMs and EDPs realizations in the log-log space is obtained. This curve is used to estimate the mean value of a parametric statistical distribution, given an IM value. The variability of this parametric distribution is calculated as the standard deviation of the IM-EDP residuals with respect to the fitted curve. Then, the probability of exceeding a specific EDP value can be estimated as a function of an IM.

5.3.1. Maximum shear strain

After performing the seismic wave propagation process, it can be estimated the time history evolution of the displacement at each interface. From this information, and the thickness of the layer, it can be calculated the evolution of the shear strain in time:

$$\gamma_i(t) = \frac{\delta_i(t) - \delta_{i-1}(t)}{h_i} \quad (4)$$

where $\delta_i(t)$ is the time-history displacement at the interface i of the soil profile; h_i represents the thickness of the layer i. Then, the maximum shear strain reached at the layer i, γ_{max_i}, can be calculated as follows:

$$\gamma_{max_i} = max(abs(\gamma_i(t))) \quad (5)$$

Finally, the maximum shear strain in the soil profile, γ_{max}, is given by:

$$\gamma_{max} = max[\gamma_{max_1}, \gamma_{max_2} \cdots \gamma_{max_n}] \quad (6)$$

Figure 10 shows 18 clouds of IM-γ_{max}, where the X-axis represents the IM and the Y-axis represents the probability of exceedance. It can be seen that $AvSv$ is the most efficient IM to predict this variable. It is worth mentioning that results in which $\gamma_{max} > 0.4\%$ have been excluded from the statistical analysis. It is because the linear equivalent method cannot properly represent the nonlinear response of the soil at these γ_{max} values.

In general, there are not significant differences between the linear and nonlinear regressions. It is worth to recall that γ_{max} has been selected as EDP since it can be used to estimate the risk to failure of soils (e.g. by the liquefaction mechanism).

By using AvSv-γ_{max} pairs, the probability of exceeding γ_{max}= 0.1% has been estimated. This damage threshold generally corresponds to a loss of stiffness around 50%, which can be seen as a severe damage state.

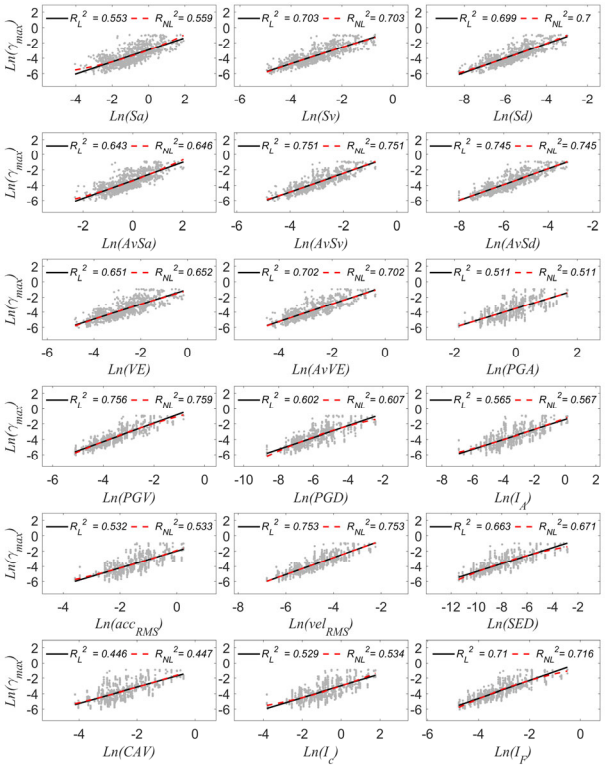

Figure 10. IM-γ_{max} clouds

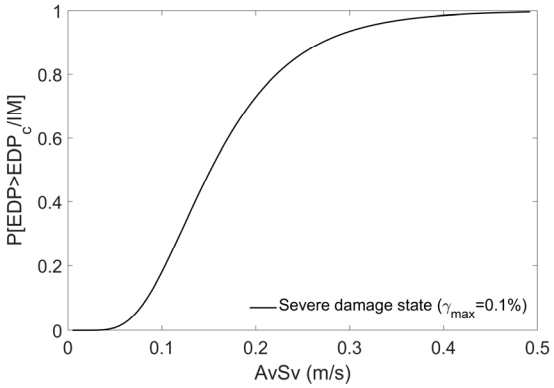

Figure 11. Fragility curve for γ_{max}= 0.1%

5.3.2. Elongation of the fundamental period

The stiffness lost by a soil profile can be estimated by analyzing the elongation of the fundamental period after propagation of seismic waves. Thus, by using the periods shown in Figure 8, the ratio between the elongated and elastic one, δT, has been defined as EDP. Figure 12 shows the 18 clouds of IM- δT pairs. In this case, the most efficient IM is $AvSd$, in which the regression has been better characterized by the quadratic model.

From AvSd-δT pairs, it has been calculated the probability of having an elongation of the fundamental period equal to 20% (See Figure 13). It can be seen that, for very low values of AvSd, the probability of reaching this level of elongation is high.

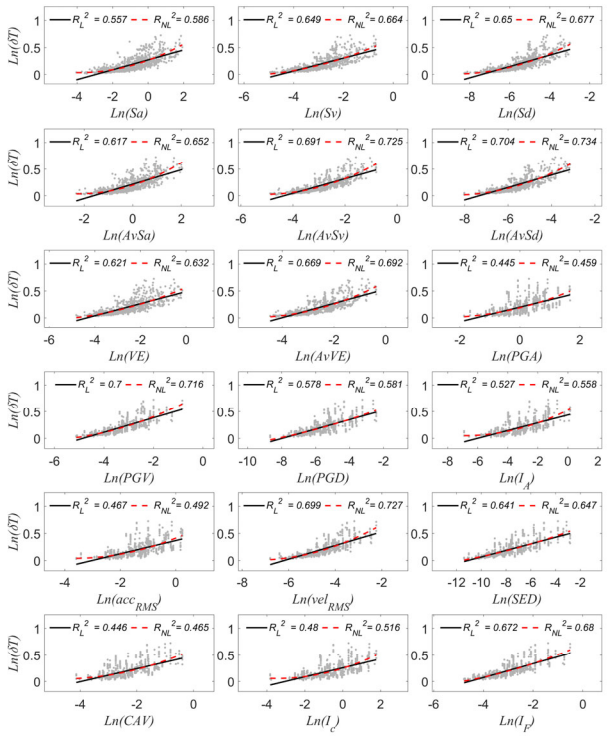

Figure 12. IM- δT clouds

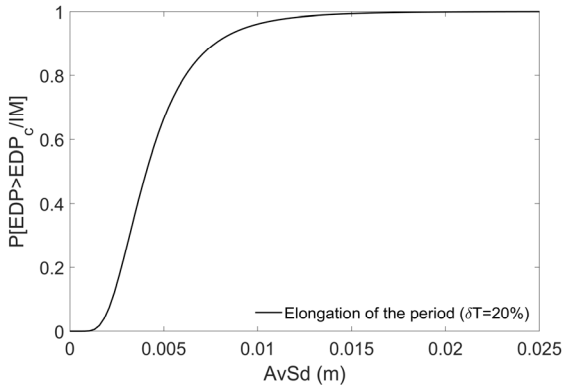

Figure 13. Fragility curve for $\delta T = 20\%$

5.3.3. Increase of damping

The degradation process induced by seismic ground motions in soil profiles generally implies an increase of damping. It is more noticeable in loose materials and can be attributed to particle rearrangement. This increase has been measured after the propagation of seismic waves through the soil profiles. It can be observed in Figure 9, where the extreme cases show increases in damping reaching values around 20%. These outcomes are probably related to the most intense ground motions of the selected set. Anyhow, these cases do not affect the statistical regressions since they have been excluded due to large shear strains. Figure 14 shows the 18 clouds of IM- ξ. As in the case of δT, $AvSd$ is the most efficient IM, yet, no significance differences have been observed between the linear and nonlinear regression.

Starting from the most correlated pairs (AvSd- ξ), it has been calculated the probability that the resulting damping exceeds 5% (See Figure 15). Again, for very low values of AvSd, the probability of reaching this damping level is high.

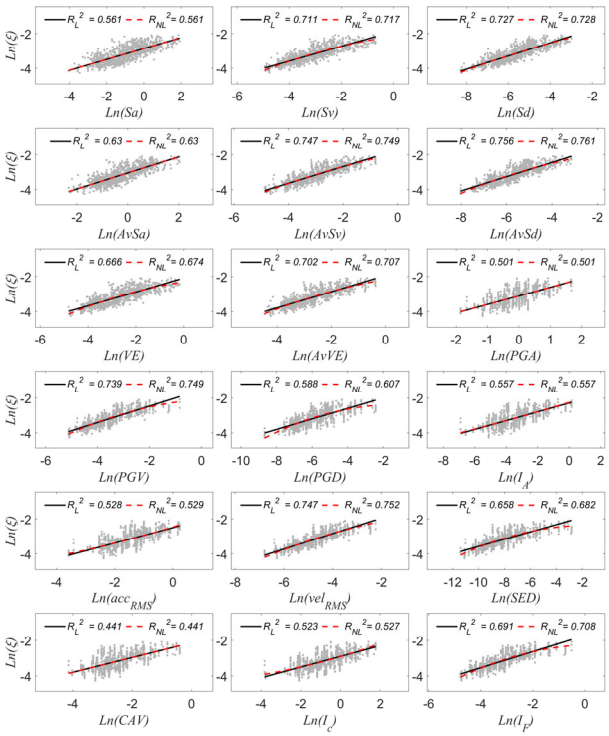

Figure 14. IM-ξ clouds

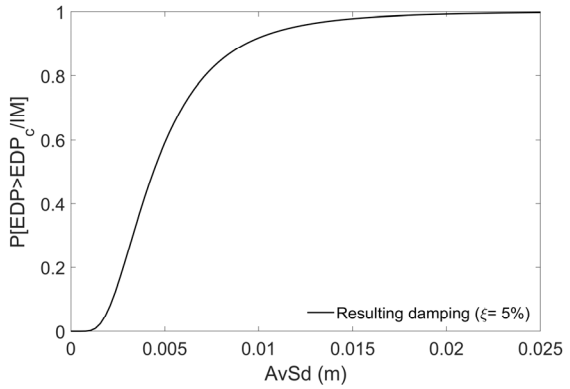

Figure 15. Fragility curve for exceeding a 5% of damping

6. Conclusion

This study highlights the importance of properly characterising site effects for robust seismic risk assessment, recognising the inherent complexity of the variables involved. The application of a computational framework for assessing the probabilistic dynamic response of soils in the Port of Barcelona, essentially using information from seismic dilatometer Marchetti test (SDMT), has provided valuable insights. The incorporation of new advances into this computational framework looks for addressing the intricate nuances of soil dynamics.

An innovative approach to seismic hazard characterisation, based on ground motion records rather than PSHA-based estimates, has been adopted to reduce the risk of underestimating seismic hazard. Quantification of inelastic ground response using the equivalent linear method further improves the accuracy of the analysis. Cloud analysis has proven effective in identifying optimal IMs for predicting specific EDPs and estimating the probability of exceeding thresholds associated with expected soil damage.

In addition, the derivation of fragility functions for each EDP provides a comprehensive understanding of the vulnerability of the soil under different conditions. The sensitivity of the dynamic response of the soil to changes in ground conditions highlights the need for careful consideration of these factors in seismic risk assessments. Overall, these results contribute to a more refined and comprehensive approach to soil dynamics analysis for improved seismic risk assessment.

Acknowledgements

The authors are grateful for the financial support of the Spanish Research Agency (AEI) through the project TED2021-132559B-I00-J-02970 and to Miguel A. Pindado and Ramón Griell of the Autoritat Portuària de Barcelona for the financial support and for providing us with the test results.

References

Alarcón, Enrique, and Mª Belén Benito Oterino. 2014. "Foreword Special Issue LORCA's Earthquake." *Bulletin of Earthquake Engineering* 12 (5): 1827–29. https://doi.org/10.1007/s10518-014-9602-4.

Amoroso, Sara, Paola Monaco, and Diego Marchetti. 2012. *Use of the Seismic Dilatometer (SDMT) to Estimate in Situ G-γ Decay Curves in Various Soil Types*.

Andrus, Ronald D., and Kenneth H. Stokoe II. 2000. "Liquefaction Resistance of Soils from Shear-Wave Velocity." *Journal of Geotechnical and Geoenvironmental Engineering* 126 (11): 1015–25. https://doi.org/10.1061/(ASCE)1090-0241(2000)126:11(1015).

Angelini, Marcos E., and Gerard B.M. Heuvelink. 2018. "Including Spatial Correlation in Structural Equation Modelling of Soil Properties." *Spatial Statistics* 25 (June): 35–51. https://doi.org/10.1016/j.spasta.2018.04.003.

API. 2014. *Recommended Practice 2GEO - Geotechnical and Foundation Design Considerations.* 22nd edition. American Petroleum Institute, Washington, RP2A-WSD.

Assimaki, Dominic, Eduardo Kausel, and Andrew Whittle. 2000. "Model for Dynamic Shear Modulus and Damping for Granular Soils." *Journal of Geotechnical and Geoenvironmental Engineering* 126 (10): 859–69. https://doi.org/10.1061/(ASCE)1090-0241(2000)126:10(859).

Atkinson, G. M., and S. I. Kaka. 2007. "Relationships between Felt Intensity and Instrumental Ground Motion in the Central United States and California." *Bulletin of the Seismological Society of America* 97 (2): 497–510. https://doi.org/10.1785/0120060154.

BSSC. 2021. *NEHRP Recommended Provisions for Seismic Regulations for New Buildings and Other Structures.* FEMA 507/513, 88. Building Seismic Safety Council .

Carrière, S. R., D. Jongmans, G. Chambon, G. Bièvre, B. Lanson, L. Bertello, M. Berti, M. Jaboyedoff, J.-P. Malet, and J. E. Chambers. 2018. "Rheological Properties of Clayey Soils Originating from Flow-like Landslides." *Landslides* 15 (8): 1615–30. https://doi.org/10.1007/s10346-018-0972-6.

Coburn, Andrew, and Robin Spence. 2002. *Earthquake Protection*. Chichester, UK: John Wiley & Sons, Ltd. https://doi.org/10.1002/0470855185.

Cruz, Cristian, and Eduardo Miranda. 2021. "Insights into Damping Ratios in Buildings." *Earthquake Engineering & Structural Dynamics* 50 (3): 916–34. https://doi.org/10.1002/eqe.3356.

Eurocode 8. 2004. *Design of Structures for Earthquake Resistance. Part 1: General Rules, Seismic Actions and Rules for Buildings.* . Vol. EN 1998-1: 2004.

Hardin, Bobby O., and Gordon D. Scott. 1967. "Erratum for 'Generalized Kelvin-Voigt Used in Soil Dynamics Study.'" *Journal of the Engineering Mechanics Division* 93 (1): 79–79. https://doi.org/10.1061/JMCEA3.0000830.

Jalayer, Fatemeh, Raffaele De Risi, and Gaetano Manfredi. 2015. "Bayesian Cloud Analysis: Efficient Structural Fragility Assessment Using Linear Regression." *Bulletin of Earthquake Engineering* 13 (4): 1183–1203. https://doi.org/10.1007/S10518-014-9692-Z.

Luzi, L, R Puglia, and E Russo. 2016. "Engineering Strong Motion Database, Version 1.0. Istituto Nazionale Di Geofisica e Vulcanologia, Observatories & Research Facilities for European Seismology." ORFEUS WG5. 2016.

Marchetti, Diego. 2018. "Dilatometer and Seismic Dilatometer Testing Offshore: Available Experience and New Developments." *Geotechnical Testing Journal* 41 (5): 20170378. https://doi.org/10.1520/GTJ20170378.

Marchetti, Silvano. 1980. "In Situ Tests by Flat Dilatometer." *Journal of the Geotechnical Engineering Division* 106 (3): 299–321. https://doi.org/10.1061/AJGEB6.0000934.

Marchetti, Silvano, Diego Marchetti, and Felipe Villalobos. 2013. "El Dilatómetro Sísmico SDMT Para Ensayos de Suelos in Situ." *Obras y Proyectos*, no. 13: 20–29. https://doi.org/10.4067/S0718-28132013000100002.

Mulargia, Francesco, Philip B. Stark, and Robert J. Geller. 2017. "Why Is Probabilistic Seismic Hazard Analysis (PSHA) Still Used?" *Physics of the Earth and Planetary Interiors* 264 (March): 63–75. https://doi.org/10.1016/j.pepi.2016.12.002.

Nakamura, Y. 1989. "A Method for Dynamic Characteristics Estimation of Subsurface Using Microtremor on the Ground Surface." *Railway Technical Research Institute/Tetsudo Gijutsu Kenkyujo* 30 (January): 25–33.

Okur, D.V., and A. Ansal. 2007. "Stiffness Degradation of Natural Fine Grained Soils during Cyclic Loading." *Soil Dynamics and Earthquake Engineering* 27 (9): 843–54. https://doi.org/10.1016/j.soildyn.2007.01.005.

Pitilakis, Dimitris, and Christos Petridis. 2022. "Fragility Curves for Existing Reinforced Concrete Buildings, Including Soil–Structure Interaction and Site Amplification Effects." *Engineering Structures* 269 (October): 114733. https://doi.org/10.1016/j.engstruct.2022.114733.

Silva, W.J., N. Abrahamson, Gabriel Toro, and C. Constantino. 1996. *Description and Validation of the Stochastic Ground Motion Model*. Pacific Engineering and Analysis.

Toro, Gabriel R. 2022. "Uncertainty in Shear-Wave Velocity Profiles." *Journal of Seismology* 26 (4): 713–30. https://doi.org/10.1007/s10950-022-10084-x.

Vanmarcke, Erik H. 1977. "Probabilistic Modeling of Soil Profiles." *Journal of the Geotechnical Engineering Division* 103 (11): 1227–46. https://doi.org/10.1061/AJGEB6.0000517.

Vargas-Alzate, Yeudy F., Jorge E. Hurtado, and Luis G. Pujades. 2022. "New Insights into the Relationship between Seismic Intensity Measures and Nonlinear Structural Response." *Bulletin of Earthquake Engineering* 20 (5): 2329–65. https://doi.org/10.1007/s10518-021-01283-x.

Zapata-Franco, A. M., Y. F. Vargas-Alzate, L. G. Pujades, and R. Gonzalez-Drigo. 2023. "Improved Intensity Measures Considering Soil Inelastic Properties via Multi-Regression Analysis." *Frontiers in Earth Science* 11 (August). https://doi.org/10.3389/feart.2023.1214536.